

Chapter 69

Experimental and Computational Evaluation of Pressure Drop and Heat Transfer Characteristics in Rectangular Channel with Helix Grooved Profile Pin Fins



J. A. Siddiqui, Subhash Lahane, A. V. Gadekar and V. L. Lokawar

Abstract The heat transfer characteristics along with pressure drop inside a rectangular channel embedded with pin fins are numerically and experimentally investigated. The geometry of the problem, meshing, and models have been solved by ANSYS Fluent 17 solver to find the optimum pin fin shape based on maximizing the heat transfer. Several geometrical shaped pin fins (i.e., circular, square threaded, and helix grooved) with the identical cross-sectional areas are compared in staggered arrangement. The Reynolds number is varied from 13,500 to 42,000 with the clearance ratio (C/H) 1 and the inter fin spacing ratio (Sy/D) 3.417. An adiabatic thermal condition is applied to the side walls of rectangular channel and a constant heat flux 3200 W/m^2 condition is applied to the heated aluminum base plate. The thermal performance analysis is made under constant air supply by air blower at inlet. Nusselt number and Reynolds numbers are considered as performance parameters. The experimental review shows that the modifications with square threaded and helix grooved geometries produce blockage to fluid flow which increases turbulence within a channel and lead to heat transfer enhancement and pressure drop. The result of staggered configuration and different geometries are also compared with the result of pin fins with solid cylindrical geometry. In terms of pressure drop and heat transfer, the square threaded cylindrical-shaped pin fin is a promising alternative configuration to conventional geometrical shape pin fins.

Keywords Pressure drop · Heat transfer · CFD · Turbulence

J. A. Siddiqui · V. L. Lokawar

Faculty of Engineering and Technology, Department of Mechanical Engineering, MGM's Polytechnic, Aurangabad 431003, Maharashtra, India

S. Lahane (✉) · A. V. Gadekar

Faculty of Engineering and Technology, Department of Mechanical Engineering, Marathwada Institute of Technology, Aurangabad 431003, Maharashtra, India
e-mail: subhashlahane@gmail.com

© Springer Nature Singapore Pte Ltd. 2020

S. Singh and V. Ramadesigan (eds.), *Advances in Energy Research, Vol. 1*, Springer Proceedings in Energy, https://doi.org/10.1007/978-981-15-2666-4_69

729

69.1 Introduction

The compactness of electronic devices leads to smaller size and formation of high amount of heat. The globally advance technology in development of high power electronic components, demand of greater functionality, larger storage space, and faster rates of information transfer for handy electronic devices have increased significantly resulting into compactness of equipment size and lead to formation of large amount of heat which reduces their life cycle. Pin fins provided on a heating surface increase the heat dissipation rate. Due to the less space availability in the system, pin fin array is one of the simplest solutions applied to heat exchanging designs.

M. Eren et al. [1] proved the pin fin geometry is an important factor which affects the friction factor in flow and heat transfer analysis. They study the effect of various grooved geometries of pin fin like cylindrical grooved and triangular-grooved pin fin with varying Reynolds number for heat transfer enhancement and friction factor. They proved that triangular-grooved pin fins give maximum heat transfer than any other pin fins. Ece Ayli et al. [2] performed computational research work with a square cross-section duct. They studied effect of Reynolds number on various geometry of pin fin with a turbulent air flow. Computational results proved that, with increase in a Reynolds number produces more turbulence. As turbulence produced due to flow blockage results in increasing Nusselt number which ultimately increases rate of heat transfer.

Hongxia Zhao [3] also performed an experimental analysis for pressure drop and friction factor. Their study was focused on varying shape of mini pin fins like circular, elliptical, square, diamond, and triangle. They also studied the effect of arrangements of pin fin like inline and staggered with the same height and transverse spacing. Their result shows that the triangular pin fins provide more heat transfer as it provides large resistance to flow in a staggered arrangement. Mi Ae Moon et al. [4] used 3D RANS analysis technique to find out maximum heat transfer with the help of fan-shaped pin fins. Experimental results proved that Average Nusselt number increases with present pin fin geometry. There is also significant pressure drop in channel due to less amount of flow resistance. Their results improved heat transfer by 22.8% at 80,000 Reynolds number.

Fengming Wang et al. [5] studied the flow and heat transfer characteristics in rectangular channel with drop-shaped pin fins. Their investigation proved that, the specific performance of drop-shaped pin fins is far better than circular pin fins. Bayram Sahin et al. [6] experimentally investigated heat transfer and pressure drop characteristics by using the Taguchi experimental design method. The experiment was performed with a Reynolds number range of 13,500 to 42,000. The experimental results proved that the factor which affects the heat transfer rate is the Reynolds number, fin spaces, and fin height. The highest heat transfer rate was observed at 42,000 Reynolds number, 3.417 fin spaces (Sy/D), and 50 mm fin height in a rectangular channel.

M.K. Chyu et al. [7] experimentally studied various geometry of pin fin like circular, cubic, and diamond-shaped pin fin arrays with staggered arrangement of

pin fins. Experimental results proved that maximum heat transfer was obtained with the diamond pin fin arrays than conventional circular pin fin arrays for the same Reynolds number. Jeng Tzer et al. [8] carried out experimental investigation of square and circular pin fin array for different arrangements. The result shows that square pin fin arrays increase Nusselt number with staggered arrangement results in high heat transfer and pressure drop. Ugur Akyo et al. [9] studied hollow rectangular geometry pin fin with a different arrangements and pitch distances. Experimental results proved that better heat transfer was obtained with the staggered arrangement due to increase in turbulence because of flow resistance. It also revealed that heat transfer increases with increase in pressure drop and friction factor because of turbulence.

N Sahiti et al. [10] continued the study of various geometries of pin fin like a NACA airfoil, lancet, drop form, ellipse, circle, and square. The aim of study was to find maximum heat transfer and friction loss within different pin fin geometries. The experimental results proved that the elliptical pin fin provides more heat transfer and its simple attractive shape provides more suitability for applications in external heat transfer. Q. Li et al. [11] investigated the heat transfer characteristic of short elliptical pin fins. Their result shows that there is a considerable heat transfer enhancement with the short elliptical pin fins than conventional circular pin fins due to staggered arrangement. It also proved that present geometry has very less flow blockage because of its elliptical shape (Table 69.1).

69.2 Experimental Set-Up and Methodology

Experimental set-up consists of a rectangular duct with an internal cross section of 250 mm × 100 mm and having the length of 1000 mm with a wall thickness of 20 mm. Rectangular duct is of wood material with very low thermal conductivity which prevents the thermal losses within a duct. The forced air is supplied at inlet of duct with the blower of 0.5 H.P. capacity and placed parallel to duct axis with a distance of 45 cm from the inlet of duct. To get streamlined air flow, convergent and divergent sections are provided with an angle of 30° at inlet and outlet as shown in Fig. 69.1. The slot of 250 mm × 250 mm is made at bottom of duct where test plate of aluminum with the pin fin arrays is inserted. Test plate is made up of same material as that of pin fin with a size of 250 mm × 250 mm and 6 mm thickness. Test plate is attached with mica plate-type electrical heater with the power output of 200 W at 38 V and a current of 5.2 A. Constant heat flux of 3200 W/m² is controlled by a variac transformer. Bottom portion of test plate is covered with glass wool to provide insulation due to thermal losses by conduction and convection. An anemometer is placed at inlet section of duct to measure mean velocity of air. The temperatures at inlet, outlet, and test sections are measured with the help of RTD temperature sensors. Differential pressure transmitter is used to measure pressure drop across the rectangular tunnel. The experiment is performed with a Reynolds number ranging from 13,500 to 42,000. The experiment is performed with a constant parameter as clearance ratio (C/H) 1 and inter fin spacing ratio (S_y/D) 3.417 as shown in Fig. 69.2.

Table 69.1 Nomenclature

A_f	Wetted surface area (m^2)	C	Distance between top of pin fin and bottom inner surface of duct (m)
A_p	Pin section area (m^2)	T	Thermodynamic temperature (K)
A	Duct Area (m^2)	u	Velocity (m/s)
Hd	Rectangular duct height (m)	m	Mass flow rate (kg/s)
B	Rectangular duct width (m)	P	Pressure (pa)
D	Diameter of pin fin (m)	ΔP	Pressure drop
H	Height of pin fin (m)	ν	Kinematic viscosity (Pa s)
D_h	hydraulic diameter (m)	k	Thermal conductivity (W/m K)
V_f	Fluid volume inside pin fins array region (m^3)	ρ	Density
p	Pitch distance (m)		
dp	Pitch diameter (m)		<i>Subscripts</i>
L	Length of pin fins array along stream line (m)	ave	Average
L_p	Pin circumference length (m)	in	Inlet
S	Distance between adjacent fins	max	Maximum
N	Number of pin fins	out	Outlet
Nu	Nusselt number	w	Wall
Re	Reynolds number	y	Stream-wise direction
q	Heat flux (W/m^2)	f	Fluid
C_p	Specific heat (J/kg K)	elect	Electrical
f	Pressure loss coefficient	cond	Conduction
h	Convective heat transfer coefficient ($W/m^2 K$)	conv	Convection
Q	Heat transfer rate (W)	rad	Radiation

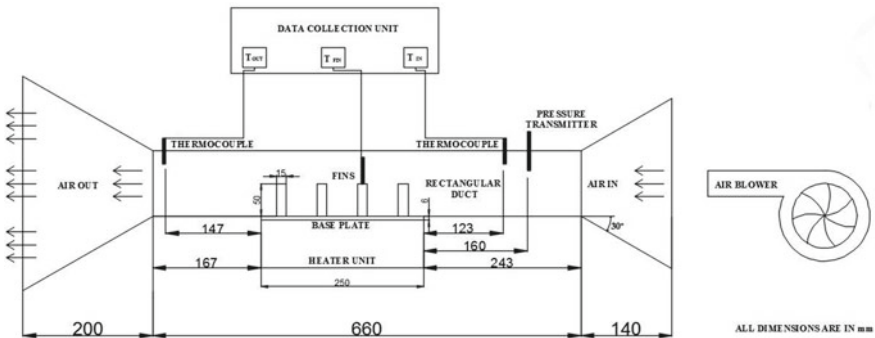


Fig. 69.1 Experimental set-up

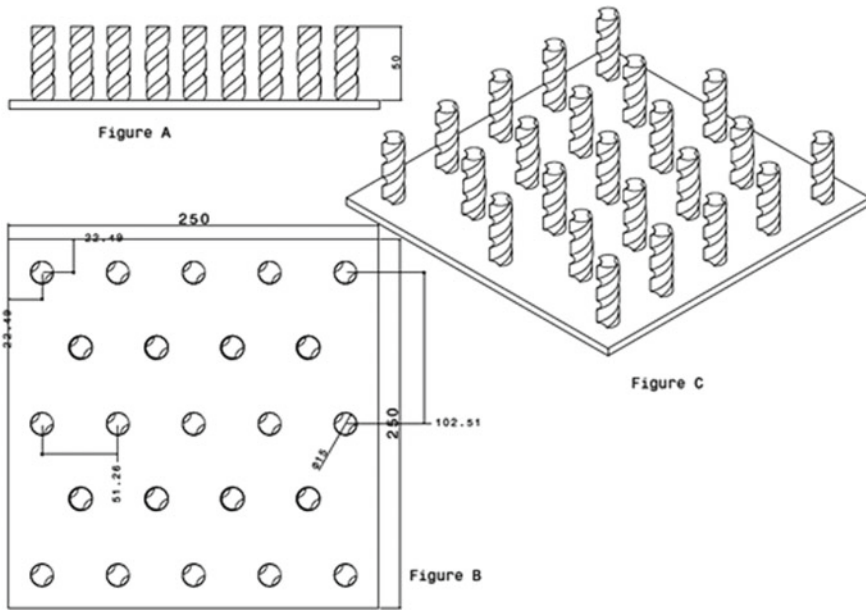


Fig. 69.2 Staggered arrangements for helix geometry

69.2.1 Pin Fin Geometry

The pin fins are located on the test plate with a staggered arrangement having an identical circular cross section of 15 mm diameter and 50 mm height. The outer part of fin is machined in the form of square thread with a pitch of 6 mm and had a 3 × 3 mm depth × width dimension as shown in Fig. 69.3a. In second case, fins with

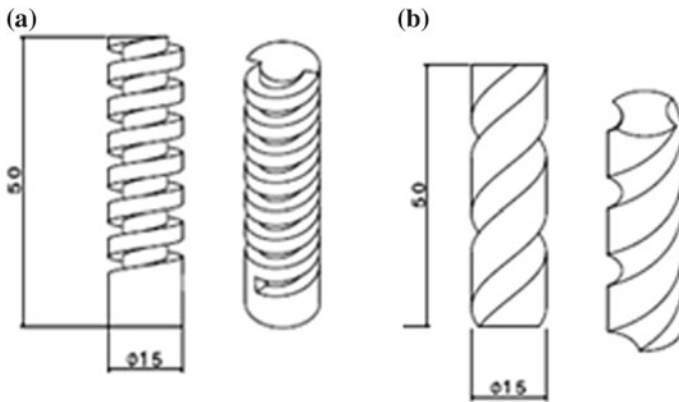


Fig. 69.3 a Square thread. b Helix

the same dimension as of square thread are machined but with a helix groove angle along the vertical axis throughout the pin fin as shown in Fig. 69.3b.

69.2.2 Computational Analysis

Experiment also performed with computational analysis to compare experimental and computational results. Computational analysis is performed with CFD ANSYS Fluent Solver of second-order up wind for the discreteness of the governing equations. Standard $k-\epsilon$ turbulence model is applied and ANSYS ICEM meshing module is used for structured mesh profiles generation. Approximately, 600,000 computational grids are involved in the entire computational domain and about 2000 grids in each pin fin. The boundary condition at inlet fluid flow temperature (T_{in}) is considered as 300 K with the no slip condition is applied to all the solid walls of rectangular duct. The constant heat flux ($q = 3200 \text{ W/m}^2$) is applied to the heated test section.

69.3 Data Analysis

69.3.1 Calculation of Heat Transfer

The convective heat transfer rate from the electrically heated test surface Q_{conv} is calculated by using Eq. (69.1),

$$Q_{conv} = Q_{elect} - Q_{cond} - Q_{rad}, \quad (69.1)$$

$$Q_{conv} = h_{avg} A_p \left[T_{wavg} - \frac{T_{f,out} - T_{f,in}}{2} \right] \quad (69.2)$$

The heat transfer from the test section by convection can be expressed by using Eq. (69.2),

Where,

$$A_p = \frac{\pi}{4} d^2 \dots \text{for cylindrical pin fin,}$$

$$A_p = \frac{\pi}{4} (dp^2 - 0.9381 \times p)^2 \dots \text{for square threadd pin fin}$$

Table 69.2 Details of different hydraulic diameter for corresponding geometries

Shape/Variable	Cylindrical	Helix grooved	Square thread
D_h (mm)	84.91810997	85.62180461	88.45430145

69.3.2 Calculation of Hydraulic Diameter (D_h)

The hydraulic diameter is defined as the ratio of the open duct volume (V_f) existing for flow to the total wetted surface area (A_f) inside the pin fin array region and can be expressed by using Eq. (69.3),

$$D_h = \frac{4V_f}{A_f}, \quad (69.3)$$

A_f is defined as the total convective heat transfer area in contact with the flowing fluid. The total convective heat transfer area includes the wall and pin areas get in touch with the fluid. It can be expressed by using Eq. (69.5),

$$V_f = BHdL - N_p A_p Hd, \quad (69.4)$$

$$A_f = 2(B + Hd)L + N_p(L_p Hd - 2A_p) \quad (69.5)$$

The Reynolds number is the ratio of inertial forces to viscous forces within a fluid which is subjected to relative internal movement due to different fluid velocities, in what is known as a boundary layer in the case of a bounding surface such as the interior of a pipe.

The Reynolds number is defined based on the hydraulic diameter considering pin fin as using Eq. (69.6),

$$Re = \frac{u_{\max} D_h}{\nu}, \quad (69.6)$$

Table 69.2 shows the details of different hydraulic diameter for corresponding geometries

69.3.3 Calculation of Convective Heat Transfer Coefficients

The local and average convective heat transfer coefficients are defined as using Eq. (69.7)–(69.8).

$$h = \frac{q}{(T_w - T_f)}, \quad (69.7)$$

$$h_{\text{avg}} = \frac{q}{(T_{\text{wavg}} - T_{\text{favg}})}. \quad (69.8)$$

T_{favg} is the total average temperature of the fluid flow, which is taken as the arithmetic average of the initial temperature (T_{fin}) and final temperature (T_{fout}), and can be expressed as Eq. (69.9),

$$T_{\text{favg}} = \frac{(T_{\text{fout}} + T_{\text{fin}})}{2}, \quad (69.9)$$

The exit temperature can be calculated as below using an energy balance across the ends of the test section as using Eq. (69.10)–(69.11),

$$T_{\text{fout}} = T_{\text{fin}} + \frac{(2qA_{\text{heater}})}{mC_p} \quad (69.10)$$

$$\text{Mass flow rate}(m) = \rho Au_{\text{in}}. \quad (69.11)$$

69.3.4 Calculation of Nusselt Number

The Nusselt number (Nu) is the ratio of convective to conductive heat transfer across the boundary. The Nusselt number is calculated experimentally and computationally for each test configuration. The relation between Nusselt number and Reynolds number for all pin fin configurations is calculated. The local and average Nusselt numbers are distinct based on the hydraulic diameter with different pin fin geometries as Eq. (69.12)–(69.13),

$$\text{Nu} = \frac{hD_h}{k} \quad (69.12)$$

$$\text{Nu}_{\text{avg}} = \frac{h_{\text{avg}}D_h}{k}. \quad (69.13)$$

69.3.5 Calculation of Friction Coefficient

The friction factor results are plotted for cylindrical, square thread, and helix grooved pin fin in a similar manner. The graph of friction factors for different Reynolds numbers is prepared. The pressure drop is calculated by using differential pressure transmitter. The pressure drop across channel and the total pressure loss coefficient or friction coefficient are calculated as Eq. (69.14)–(69.15),

$$\Delta P = (P_{in} - P_{out}), \tag{69.14}$$

$$F = \frac{P_{in} - P_{out}}{\frac{1}{2}\rho\mu_{in}^2} \tag{69.15}$$

69.4 Results and Discussion

69.4.1 Heat Transfer Characteristics

The Nusselt number is calculated for each test configuration. Figure 69.4 shows the combined computational and experimental results between Nusselt number and Reynolds number for all pin fin configurations, result shows that the average Nusselt number increases with increase in Reynolds number as high Reynolds number produces the turbulence. Average Nusselt number reaches maximum value at 42,000 Reynolds number and gives maximum value for square thread pin fins. The result shows that there is a variation in computational and experimental results about 11%. These observations led to the conclusion that during the flow system change, there is a sharp increase in Nu for all configurations. The square threaded pin fin has the maximum Nu among all morphologies.

The local heat transfer is significantly enhanced in the area near the pin fin circumferences for all the three different cases. Figure 69.5 shows the computational results of temperature distribution and local Nusselt number distributions across the pin fins at the heated area of base plate with different types of pin fin arrays at 42,000 Reynolds number.

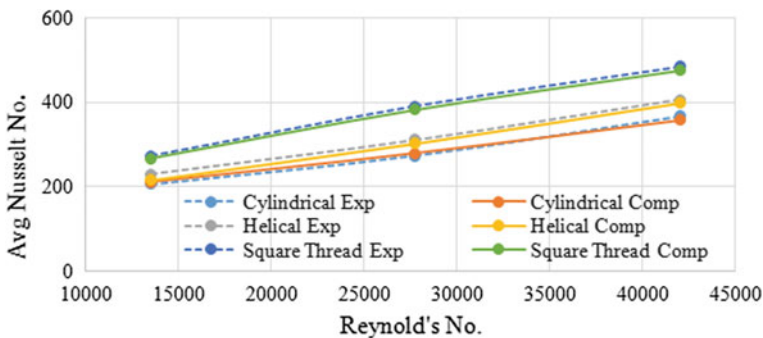


Fig. 69.4 Experimental and computational results of Nu_{avg} versus Re

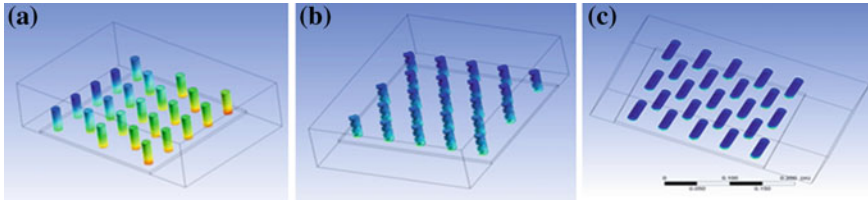


Fig. 69.5 Temperature distribution of pin fins at Re 42,000 **a** cylindrical. **b** helix grooved. **c** square thread

The result proved that the pin fins of grooved shape affect the temperature distribution. The helically grooved pin fins give more developed flow than any other fins which gives more efficient heat transfer. Due to the strong turbulence and recirculation flow within helically grooved pin fin arrays, it gives high heat transfer coefficient than conventional cylindrical pin fins. Turbulence formed due to staggered arrangement and grooved geometry even produces high heat transfer coefficient. As base material and pin fin material is aluminum, it produces same temperature which enhances the heat transfer with minimum losses. Figure 69.5 shows the temperature distribution at 42,000 Reynolds number. It shows approximately same temperature distribution at inlet for all three cases but produces considerable difference in temperature distribution at outlet which is higher in case of helically grooved pin fins, resulting in fully turbulent flow and high heat transfer coefficient.

69.4.2 Pressure Drop and Friction Characteristics

The pressure drops in the tunnel without fins is too small that it could not be deliberate by the pressure transducer. This resulted from smaller length of the test section and smaller roughness of the rectangular duct. The experimental pressure drops over the test section in the finned duct is calculated under the heated flow circumstances. Figure 69.6a shows the pressure distribution at inlet for the helix grooved pin fins at Re 13,500. Result shows that pressure at inlet increases with increase in Reynolds number and creates turbulence across the pin fin array. The increase in the turbulence increases friction factor and leads to cooling of pin fin array. Figure 69.6b shows the pressure distribution at outlet for the helix grooved pin fins. Due to turbulence created across the pin fin array pressure at outlet decreases and pressure drop across the rectangular tunnel increases. In case of square threaded pin fin, pressure drop across the rectangular tunnel increases more than circular and helix grooved pin fins.

The specific friction loss of square threaded pin fin is more than that of helical grooved pin fins and cylindrical solid pin fins, which indicates that the square threaded pin fins are more advantageous than the others.

Figure 69.7 shows combined computational and experimental results of variation of friction factor with different Reynolds number. The result shows that the friction

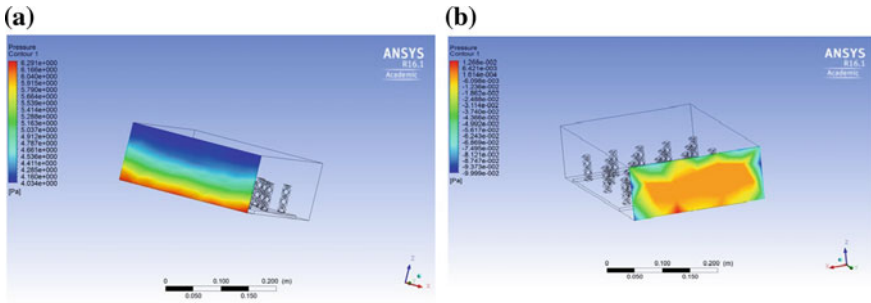


Fig. 69.6 Pressure distribution for helix grooved pin fins a Inlet. b Outlet

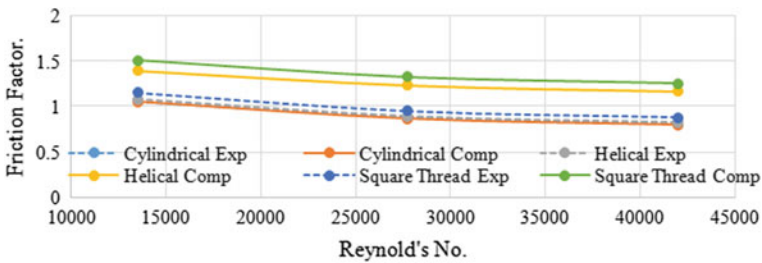


Fig. 69.7 Experimental and computational results of f versus Re

factor is maximum for square thread pin fin at 13,500 Reynolds number. It decreases with increase in Reynolds number. The values of computational results are higher than that of the experimental results. Computationally, square thread gives more heat transfer than other pin fin but the values of helix pin fin for computational results are more than values of square thread geometry for experimental results. This problem may occur due to errors within the parameters measurement and intrinsic numerical errors due to numerical operations such as error truncation.

Figure 69.8a shows the velocity distribution for circular pin fin at Re 42,000. The

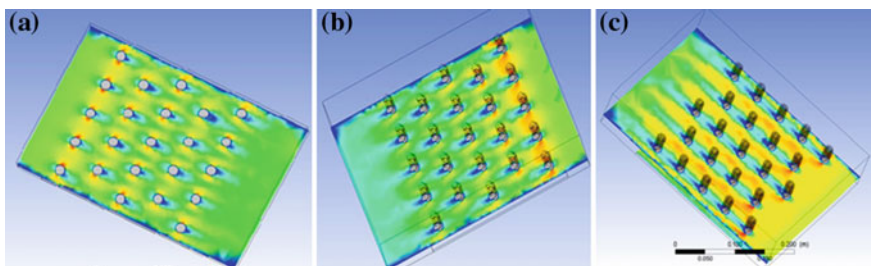


Fig. 69.8 Velocity distribution of pin fins at Re 42,000 a cylindrical. b helix grooved. c square thread

result shows that the flow is somewhat straight for circular pin fins and produces less friction. The turbulence also in this area is less. Figure 69.8b shows the velocity distribution for helix grooved pin fin at Re 42,000. The result shows that turbulence increases near the pin fin base which increases the heat transfer. Figure 69.8c shows the velocity distribution for square threaded pin fin at Re 42,000. The result shows that the maximum turbulence is created in square thread pin fin. There is maximum friction factor and heat transfer increases in a square threaded pin fin as compared to helix grooved and cylindrical pin fins. It can readily be seen that the friction factor varied greatly in connection to changes in Reynolds number. There is a sharp increase in friction factor for square threaded geometry during the changing of the flow. This increment is smoother for circular pins.

69.5 Conclusions

The conclusions from results obtained are summarized as:

1. The average increase in heat transfer coefficient of square threaded (27.50%) and helical grooved pin fin (10.86%) is greater than that of circular pin fins because of turbulence created within pin fin arrays.
2. The average increase in Nusselt number of square threaded (32.80%) and helical grooved pin fin (11.78%) is greater than that of circular pin fins as square threaded geometry provides more blockages to fluid flow.
3. The average increase in friction factor with square threaded (8.50%) and helical grooved pin (1.64%) geometries as compared to cylindrical and friction factor decreases with increase in Reynolds number.
4. Nusselt number increases with increase in Reynolds number as it produces more turbulence.
5. Computational results are in good conformity with the experimental findings and vary between 15 and 20%. Variations in the results are because of experimental errors. Therefore, computational fluid dynamics analysis is helpful for predicting heat transfer characteristics of the turbulent flow of square threaded and helical grooved pin fins.

References

1. M. Eren, S. Caliskan, Effect of grooved pin fins in a rectangular channel on heat transfer augmentation and friction factor using Taguchi method. *Int. J. Heat Mass Transf.* **102**, 1108–1122 (2016)
2. Ece Ayli, Ozgur Bayer, Selin Aradag, Experimental investigation and CFD analysis of rectangular profile FINS in a square channel for forced convection regimes. *Int. J. Therm. Sci.* **109**, 279–290 (2016)

3. Hongxia Zhao, Zhigang Liu, Chengwu Zhang, Ning Guan, Honghua Zhao, Pressure drop and friction factor of a rectangular channel with staggered mini pin fins of different shapes. *Exp. Thermal Fluid Sci.* **71**, 57–69 (2016)
4. MiAe Moon, Kwang Yong Kim, Analysis and optimization of fan shaped pin fin in a rectangular cooling channel. *Int. J. Heat Mass Transf.* **72**, 148–162 (2014)
5. Fengming Wang, Jing Zhou Zhang, Suo fang Wang, Investigation on flow and heat transfer characteristics in rectangular channel with drop shaped pin fins. *Propul. Power Res.* **1**(1), 64–70 (2012)
6. Bayram Sahin, Alparslan Demir, Performance analysis of a heat exchanger having perforated square fins. *ELSEVIER, Appl. Therm. Eng.* **28**, 621–632 (2008)
7. M.K. Chyu, C.H. Yen, S. Siw, Comparison of heat transfer from staggered pin fin arrays with circular, cubic and diamond shaped elements. *ASME Turbo Expo (GT2007 28306)* (2007)
8. Jeng Tzer Ming, Tzeng Sheng Chung, Pressure drop and heat transfer of square pin fin arrays in inline and staggered arrangements. *Int. J. Heat Mass Transf.* **50**, 2364–2375 (2007)
9. Ugur Akyo, Kadir Bilen, Heat transfer and thermal performance analysis of a surface with hollow rectangular fins. *Appl. Thermodyn. Eng* **26**, 209–216 (2006)
10. N. Sahiti, A. Lemouedda, D. Stojkovic, F. Durst, E. Franz, Performance comparison of pin fin in duct flow arrays with various pin cross sections. *Appl. Therm. Eng.* **26**, 1176–1192 (2006)
11. Q. Li, Z. Chen, U. Flechtner, H.J. Warnecke, Heat transfer and pressure drop characteristics in rectangular channels with elliptic pin fins. *Int. J. Heat Fluid Flow* **19**(3), 245–250 (1998)